

Stochastic Modelling of Random Access Memories Reset Transitions

M. Carmen Aguilera-Morillo^a, Ana M. Aguilera^{b,*}, Francisco
Jiménez-Molinos^c, Juan B. Roldán^c

^a*Department of Statistics. University Carlos III of Madrid, Spain*

^b*Department of Statistics and O.R. and IEMath-GR, University of Granada, Spain*

^c*Department of Electronics and Computer Technology. University of Granada, Spain*

Abstract

Resistive Random Access Memories (RRAMs) are being studied by the industry and academia because it is widely accepted that they are promising candidates for the next generation of high density nonvolatile memories. Taking into account the stochastic nature of mechanisms behind resistive switching, a new technique based on the use of functional data analysis has been developed to accurately model resistive memory device characteristics. Functional principal component analysis (FPCA) based on Karhunen-Loève expansion is applied to obtain an orthogonal decomposition of the reset process in terms of uncorrelated scalar random variables. Then, the device current has been accurately described making use of just one variable presenting a modeling approach that can be very attractive from the circuit simulation viewpoint. The new method allows a comprehensive description of the stochastic variability of these devices by introducing a probability distribution that allows the simulation of the main parameter that is employed for the model implementation. A rigorous description of the mathematical theory behind the technique is given and its application for a broad set of experimental measurements is explained.

Keywords: Functional data, Karhunen-Loève expansion, Penalized splines, Resistive switching, Resistive memories, Device variability

*Corresponding author

Email address: aaguiler@ugr.es (Ana M. Aguilera)

1. Introduction

Since the presentation of Moore's law fifty years ago [1], the scaling of electronic devices has been increasing continuously till now. Gordon Moore observed that the number of components within integrated circuits double approximately every 18 months. Since that time, in the sixties, the production lines in the electronic industry have been working under pressure with the objective of fulfilling Moore's law. The most important internal computer circuits: microprocessors and memories also have fallen under the influence of the scaling trend imposed by this law [1, 2].

The reduction of semiconductor devices is not an easy task, the path of scaling is flooded with physical and technological hurdles that sometimes can not be solved. This situation is found in different facets of the integrated circuit industry, in particular in the non-volatile memory realm. The basic components found in non-volatile memory chips, floating-gate transistors, are thought to be facing important limits [2]; therefore, other emerging technologies are under study both in the industry and the academia. Among them there can be found resistive switching (RS) memories [2, 3, 4, 5], phase change memories (PCM) [6] and Spin-transfer torque random access memories (STT-RAM) [7].

RRAMs can store information without the need of a power source when they are switched off. These devices, with an operation based on resistive switching mechanisms, show interesting characteristics such as fast switching speed, endurance, low power operation and compatibility with current complementary metal-oxide-semiconductor CMOS technology [3, 8]. Because all this, they are considered the most promising future technology for non-volatile memories [2, 5, 4].

Each generation of devices developed in the microelectronic industry needs to be completely characterized; i.e., the electric currents, capacitances and other magnitudes have to be measured and modeled in such a way that they can be

calculated versus the voltages applied at their terminals by means of analytical equations. These analytical expressions are employed in circuit simulators, using also Kirchhoff's laws, to design electronic circuits. A set of equations and the corresponding fitting parameters that characterize an electron device for circuit simulation is known as a compact model and they are under continuous development due to new physical effects that show up as device dimensions are reduced and new materials and technological processes are employed in their fabrication.

A compact model is essential for the introduction of a technology since the fabrication of new integrated circuits is extremely complicated if previous circuit simulations can not be performed. Although several authors have published models for RRAMs [9, 10, 11, 12], there is a long way to go in this field, mostly taking into account the variety of physical mechanisms employed to explain the physics behind the operation of dozens of different RRAMs to date [3]. It is well known that the mechanisms behind resistive switching, the core of RRAM operation, are stochastic [4, 5]. The formation of conductive filaments that help to drastically change the resistance of the device, from a High Resistance State (HRS) to a Low Resistance State (LRS) is known as a set process, the reverse transition is known as a reset process; in this latter case, the conductive filament is destroyed. These filaments are formed by the random clustering of metallic ions or oxygen vacancies [4, 5]. That is why a mathematical model and an analysis tool that allow the description of the current-voltage curves by considering the stochastic nature of the device operation are highly desirable. The present study addresses this problem by proposing a novel approach based on Functional Data Analysis (FDA) methodologies for modeling and reconstruction of RRAM current-voltage curves. As far as we know, it is the first time that FDA is used to model these type of reset/set stochastic processes. The interested reader is referred to [13, 14, 15, 16, 17] for a detailed study of the theoretical, computational and applied aspects of the most basic FDA statistical methods.

FDA is a very successful subject of statistical research where the data units are functions of a continuous domain instead of vectors as in classical multi-

variate analysis. In the most usual case, the functions are curves defined on a real interval of time or other continuous magnitude as voltage in the case of RRAM reset/set processes. The dimension reduction technique Functional Principal Component Analysis (FPCA) is performed in this paper to provide an approximated orthogonal decomposition of the stochastic process generating the current-voltage curves in terms of a finite set of uncorrelated scalar random variables that explain the main features of process variability [18]. FPCA is based on the well known Karhunen-Loève expansion introduced by [19, 20]. FDA techniques have been successfully applied in chemical, physics, engineering and mathematics, including many other interdisciplinary areas [21, 22, 23, 24] [25, 26, 27, 28].

In our analysis, experimental measurements from a sample of reset cycles have been employed to formulate and estimate the statistical model in a comprehensive and coherent manner. In FDA, the first step, previous to apply a concrete methodology, is to reconstruct the mathematical shape of the curves over their entire domain. The problem related with having discrete observations of the reset process with different domains among sample curves (their domains are upper bounded by the reset voltage) is solved by a new approach based on synchronization of the observed curves in a common interval. Then, FPCA is estimated by using P-spline smoothing in terms of basis representation with B-spline functions [29]. In this way some of the well-known FDA features are employed here to their full extent in order to capture the random characteristics of RRAM operation. The most important goal in this paper is to study and model important patterns of variability among the data (the goals of functional data analysis are essentially the same as those of any other branch of statistics [13], Chap. 1).

The manuscript is organized as follows. In Section 2, we describe the technological details of the fabricated devices and observational data. In Section 3 the features of the modeling procedure based on FPCA are explained. In Section 4 the main results and the corresponding discussion are given. Finally, in Section 5 we wrap up the contents presented along the paper.

2. Device fabrication and observational data

The devices studied were fabricated at the IMB-CNM (CSIC) in Barcelona. They are based on a $\text{Ni}/\text{HfO}_2/\text{Si} - n^+$ structure, the dielectric layer was 20nm thick; other details of the fabrication process and measurement setup are given in [30]. In these memories, conduction takes place inside conductive filaments (CFs) that are formed and destroyed within the RS device operation [30, 31].

In this work, only experimental measurements are used. Nevertheless, simulated results can also be used in future developments since we have implemented a simulation tool that accounts for the main physical effects involved in RRAM operation [32, 33, 34].

A few current-voltage curves corresponding to several set-reset cycles are shown in Figure 1. Reset curves are shown in red lines while set curves are given in blue lines. These curves correspond to different cycles from a set-reset series of three thousands cycles. It can be seen that the curves are different in all the cases, this is due to the stochastic nature of the processes behind the conductive filament formation that determines the device resistance, i.e., the ratio between the device voltage and the corresponding current [2, 5, 4, 32].

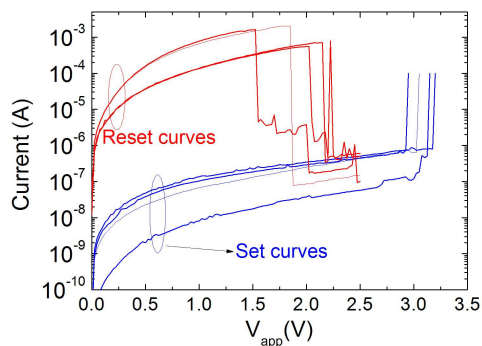


Figure 1: Experimental current versus applied voltage for several set/reset transitions in a long set-reset series for devices based on a $\text{Ni}/\text{HfO}_2/\text{Si} - n^+$ structure. Although the Ni electrode had a negative voltage applied while the substrate was grounded [30], we have considered absolute values for the applied voltage in order to ease the modeling process for curves in the first quadrant. The curves have been plotted on a logarithmic scale for the current.

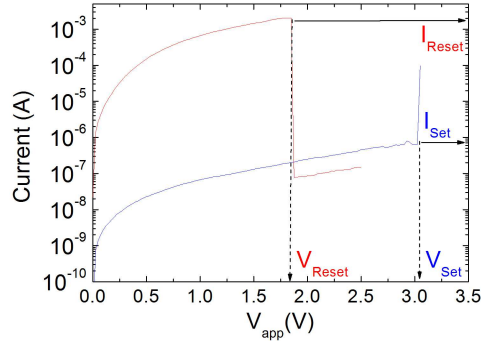


Figure 2: Experimental current versus applied voltage for a set and reset transitions for a device based on a Ni/HfO₂/Si - n⁺ structure. The (V_{Reset} , I_{Reset}) and (V_{Set} , I_{Set}) points are highlighted.

Two of the curves plotted above have been isolated in Figure 2. The V_{Reset} and I_{Reset} points are marked for the reset curve (red line). For any reset curve, these magnitudes represent the reset voltage and reset current linked to the rupture of the conductive filament [30, 31]. So the reset point is determined by the sudden drop of the current and at this point the device enters the high resistance state because the resistance of the conductive filament is much lower than the dielectric resistance. The V_{Set} and I_{Set} points are also marked for the set curve (blue line). For any set curve, these magnitudes mark the set voltage and set current where the creation of the conductive filament takes place. The filament formation makes the RRAM resistance greatly diminish because of the low resistance of the conductive filament.

As it will be shown in the next section, the reset voltage is a key parameter for our modeling procedure, since all the reset curves studied are defined between zero and the corresponding V_{Reset} , which is different among them. Because of this, all the curves are first normalized in the interval [0,1]. Then, the other FDA steps are performed.

3. Functional data analysis

As stated in the introduction, Functional Data Analysis is performed in this paper for modeling and explaining the stochastic variability of the curves of evolution of electric current (I) in terms of voltage (V) from a sample of reset cycles in Resistive Random Access Memories (RRAMs). Let us denote by $\{I(v) : v \in T\}$ the stochastic process of evolution of current in terms of voltage in a real interval T .

In order to reduce the dimension and explain the main features and modes of variation of the current-voltage reset process, the present study perform a new approach based on functional principal component analysis (FPCA) that was introduced by [35, 18] as a generalization of multivariate principal component analysis to the case of a continuous-time stochastic processes. FPCA is based on the well known Karhunen-Loève expansion (KLE) that makes an orthogonal decomposition of the process in terms of uncorrelated random variables and deterministic functions. This method was first introduced as harmonic analysis of a stochastic process. Asymptotic theory and statistical inference on FPCA were developed in [36].

3.1. Karhunen-Loève expansion

Let us suppose that $\{I(v)\}$ is a second order stochastic process defined on a probabilistic space (Ω, A, P) , continuous in quadratic mean and whose sample functions belong to the Hilbert space $L^2[T]$ of the square integrable functions on T , with the natural inner product defined by

$$\langle f|g \rangle := \int_T f(v)g(v)dv \quad \text{for all } f, g \in L^2[T].$$

The covariance operator \mathcal{C} of $\{I(v)\}$ is a positive autoadjoint compact operator defined on $L^2[T]$ by

$$\mathcal{C}(f(v)) := \int_T C(v, u)f(u)ds,$$

with kernel the covariance function $C(v, u)$. Then, the spectral representation of \mathcal{C} provides the following orthogonal decomposition of the process, known as

Karhunen-Loève orthogonal expansion [20, 19]:

$$I(v) = \mu(v) + \sum_{j=1}^{\infty} f_j(v)\xi_j, \quad (1)$$

where $\{f_j\}$ is the orthonormal family of eigenfunctions of the covariance operator \mathcal{C} associated with its decreasing sequence of non null eigenvalues $\{\lambda_j\}$, that is

$$\mathcal{C}(f_j(v)) = \int_T C(v, u)f_j(u)du = \lambda_j f_j(v), \quad v \in T,$$

and $\{\xi_i\}$ is the family of uncorrelated zero-mean random variables defined by

$$\xi_j := \int_T f_j(v)(I(v) - \mu(v))dv.$$

The random variable ξ_j is called the j th principal component and has the maximum variance λ_j out of all the generalized linear combinations of $I(v)$ which are uncorrelated with ξ_k ($k = 1, \dots, j-1$). Similarly, f_j is called the j th principal weight function or harmonic factor.

Taking into account that the total variance of $\{I(v)\}$ is given by

$$V := \int_T C(v, v)dv = \sum_{j=1}^{\infty} \lambda_j,$$

then the ratio λ_j/V is the variance explained by the j th component.

In addition, the series (1) truncated in the q th term is the best approximation of the process (in the least-squares sense) by a sum of q quasi-deterministic terms [37]. Therefore the process admits the following principal component reconstruction:

$$I(v)^q = \mu(v) + \sum_{j=1}^q f_j(v)\xi_j,$$

in terms of the first q principal components so that the sum of the variances explained by them is as close as possible to one.

3.2. Sample FPCA

In practice, to estimate the functional principal components and weight functions we have a random sample of functional data that consists of n reset curves denoted by

$$\{I_i(v) : i = 1, \dots, n; v \in [0, V_{i-reset}]\},$$

where $V_{i-reset}$ is the voltage to reset. In addition, the data consist of discrete observations of each reset curve $I_i(v)$ at a finite set of current values until the $V_{i-reset}$ point. Concretely, each curve $I_i(v)$ is observed at $k_i = V_{i-reset} * 10^3$ discrete equally spaced sampling points $v_j = j * 10^{-3}$ ($j = 1, \dots, k_i$).

In this context, the estimation of FPCA presents two important problems. On one hand, the reset curves are not defined on the same domain because the voltage to reset is different among cycles. On the other hand, we only have discrete observations of each reset curve at a finite set of current values until the V_{reset} point. To solve these problems we propose a novel FDA approach based on three main steps:

1. Registration of the reset curves in the interval $[0,1]$.
2. Reconstruction of the reset curves by P-spline smoothing on the registered data.
3. Functional PCA of the basis representation of reset curves in terms of P-splines.

Let us now briefly summarize each of these steps.

Registration

Let us observe that the reset curves have different domains because the voltage to reset is different among cycles. In this case, the first step in FDA is curve registration (transforming curves by transforming their arguments (see [13], Chap. 7, for a detailed description). In this paper we propose to do it in the simplest way that consists of transforming the domain $[0, V_{i-reset}]$ of each reset curve in the interval $[0, 1]$ by the function $v/V_{i-reset}$. Then, FDA methodologies will be performed on the synchronized curves given by

$$I_i^*(u) := I_i(u * V_{i-reset}) \quad \forall u \in [0, 1],$$

so that

$$I_i(v) = I_i^*(v/V_{i-reset}) \quad \forall v \in [0, V_{i-reset}].$$

This way, for each curve we have a new set of arguments in the interval $[0,1]$ given by

$$u_{ij} := \frac{v_j}{V_{i-reset}} = \frac{j}{k_i} \quad (j = 1, \dots, k_i).$$

This means that the sampling points where the registered curves are observed are different not only in number but also in position.

Basis representation and smoothing

In order to reconstruct the true functional form of registered reset curves we will assume that they belong to a finite-dimension space spanned by a basis $\{\phi_1(t), \dots, \phi_p(t)\}$, so that they are expressed as

$$I_i^*(u) = \sum_{j=1}^p a_{ij} \phi_j(u), \quad i = 1, \dots, n. \quad (2)$$

The selection of the basis and its dimension p is crucial and must be done according to the characteristics of the curves. Useful basis systems are Fourier basis for periodic data, B-spline basis for non-periodic smooth data with continuous derivatives up to certain order, and wavelet basis for data with a strong local behavior whose derivatives are not required [14, 38, 39]. Assuming that the reset curves are smooth and observed with error

$$I_{ij}^* = I_i^*(u_{ij}) + \epsilon_{ij} \quad j = 0, 1, \dots, k_i, i = 1, \dots, n,$$

least squares approximation with B-splines basis is an appropriate choice to approximate the basis coefficients a_{ij} .

A B-spline basis of order $p+1$ (degree p) generates the space of the splines of the same degree, defined as curves consisting of piecewise polynomials of degree p that join up smoothly at a set of definition knots with continuity in their derivatives up to order $p-1$. A detailed study of these bases can be seen in [40]. A pioneer work on data analysis with splines was developed by [41].

In this paper, the iterative definition of B-splines introduced by [42] is considered. Denoting the definition knots by $t_0 < \dots < t_m$, and extending this partition of the domain as $t_{-p} < \dots < t_{-2} < t_{-1} < t_0 < \dots < t_m < t_{m+1} <$

$t_{m+2} < \dots < t_{m+p}$, the basis of B-splines of order $p + 1$ (degree p) is iteratively defined by

$$B_{j,p+1}(t) := \frac{t - t_{j-2}}{t_{j+p-2} - t_{j-2}} B_{j,p}(t) + \frac{t_{j+p-1} - t}{t_{j+p-1} - t_{j-1}} B_{j+1,p}(t)$$

$$p = 1, 2, \dots; j = -1, 0, \dots, m - p + 4,$$

with

$$B_{j,1}(t) := \begin{cases} 1 & t_{j-2} \leq t < t_{j-1} \\ 0 & \text{otherwise} \end{cases}, j = -1, 0, 1, \dots, m + 4.$$

The curves fitted by ordinary least squares approximation in terms of B-spline basis are known as regression splines and their main problem is that they don't control the degree of smoothness. Penalized spline smoothers are usually considered to solve this problem by introducing a penalized least squares approach that measures the roughness of the curves. Smoothing splines (continuous roughness penalty) were applied to improve the extraction of threshold voltage in MOSFETs transistors ([43, 44]). In this paper, P-splines (discrete roughness penalty) are used for reconstructing the reset curves. They measure the roughness of the curves by summing squared d-order differences between adjacent B-splines and their main advantage is that the number of knots is not so determinant as in regression splines and can be easily compute ([45, 46]). As the reset curves are smooth enough to ensure an accurate spline approximation, an appropriate alternative to P-splines could be using regression splines and choosing the dimension of the B-spline basis by cross-validation.

For each reset curve, the basis coefficients of the penalized spline smoother in terms of B-spline basis functions are computed by minimizing the penalized least squares error

$$PMSE_d(a_i | I_i^*) := (I_i^* - \Phi_i a_i)' (I_i^* - \Phi_i a_i) + \lambda a_i' P_d a_i,$$

with $I_i^* = (I_{i1}, I_{i2}, \dots, I_{ik_i})'$ being the vector of discrete measures of the registered curve $I_i^*(u)$, $\Phi_i := (\phi_j(u_{ij}))_{k_i \times p}$ being the matrix of values of the basis

functions at the sampling points and $P_d := (\Delta^d)' \Delta^d$ with Δ^d being the matrix representation of the d-order difference operator.

Then, the B-spline basis coefficients for each curve are given by

$$\hat{a}_i = (\Phi_i' \Phi_i + \lambda P_d)^{-1} \Phi_i' I_i^*.$$

In general, the knots of a P-spline must be equally spaced and its number sufficiently large to fit the data and not so large that computation time is unnecessarily big. There are some important choices related to the P-spline fitting: the smoothing parameter, the order of the penalty, the degree of the B-spline basis and the number of knots. The simplest and most usual choice for these parameters that should work well in most applications is using cross-validation for chosen the smoothing parameter, a quadratic penalty, cubic splines and one knot for every four or five observations up to a maximum of about 40 knots (see [47] for a comparative study of the performance of regression splines, smoothing splines and P-splines on simulated and real data).

In order to select the same smoothing parameter for all the n sample paths we propose to minimize the mean of the leave-one-out cross validation errors over all sample curves.

The leave-one-out cross validation (CV) method consist of selecting the smoothing parameter λ that minimizes

$$CV(\lambda) = \frac{1}{n} \sum_{i=1}^n CV_i(\lambda),$$

where

$$CV_i(\lambda) = \sqrt{\sum_{j=0}^{k_i} (I_{ij}^* - \hat{I}_{ij}^{*-j})^2 / (k_i + 1)},$$

with \hat{I}_{ij}^{*-j} being the values of the i -th sample path estimated at time t_{ij} avoiding the j -th time point in the iterative estimation process.

A computationally simplest approach very used in the literature about smoothing splines is generalized cross-validation (GCV) [48]. The GCV method consist

of selecting λ which minimizes

$$GCV(\lambda) = \frac{1}{n} \sum_{i=1}^n GCV_i(\lambda),$$

where

$$GCV_i(\lambda) = \frac{(k_i + 1)MSE_i(\lambda)}{[\text{trace}(I - H_i(\lambda))]^2},$$

with $MSE_i(\lambda) = \frac{1}{n} \sum_{j=0}^{k_i} (I_{ij}^* - \hat{I}_{ij}^*)^2$, $H_i(\lambda) = \Phi_i (\Phi_i' \Phi_i + \lambda P_d)^{-1} \Phi_i'$, Φ_i being the B-spline basis evaluated at the observation knots and P_d the discrete penalty matrix.

As alternative to the methodology exposed above, the relation between P-splines and BLUP (best linear and unbiased predictor) in a mixed model allows, in some cases, to use the existing methodology in the field of mixed models in order to select a common smoothing parameter for all curves. In fact, this idea is based on writing a non-parametric or semi-parametric model as a mixed model [49, 50]. Using the mixed model framework it is possible to estimate the smoothing parameter together with the rest of the parameters of the model, instead of using cross validation algorithms. The standard method for the estimation of variance components in mixed models is the restricted maximum likelihood method (REML).

Sample estimation

The sample estimate of the j -th principal component score associated with the registered reset process is given by

$$\hat{\xi}_{ij}^* := \int_0^1 (I_i^*(u) - \bar{I}^*(u)) \hat{f}_j^*(u) du, \quad i = 1, \dots, n,$$

where $\bar{I}^*(u)$ is the sample mean function

$$\bar{I}^*(u) := \frac{1}{n} \sum_{i=1}^n I_i^*(u),$$

and the weight functions \hat{f}_j^* are the eigenfunctions of the sample covariance operator \hat{C}^* . That is, the solutions to the second order eigenequation

$$\hat{C}^*(\hat{f}_j^*)(u) = \int_0^1 \hat{C}^*(u, v) \hat{f}_j^*(v) dv = \hat{\lambda}_j^* \hat{f}_j^*(u),$$

PC	Percentage of variance
1	97.2723
2	2.3562
3	0.2344
4	0.0989

Table 1: Percentages of variance explained by the first four principal components of P-spline smoothing on the registered reset curves.

where $\hat{C}^*(u, v)$ is the sample covariance function

$$\hat{C}^*(u, v) := \frac{1}{n-1} \sum_{i=1}^n (I_i^*(u) - \bar{I}^*(u))(I_i^*(v) - \bar{I}^*(v)).$$

Then, an approximation of the sample curves is computed by truncating the KLE in terms of the first q principal components

$$I_i^{*q}(u) = \bar{I}^*(u) + \sum_{j=1}^q \hat{\xi}_{ij}^* \hat{f}_j^*(u),$$

whose explained variance is given by $\sum_{j=1}^q \hat{\lambda}_j^*$.

Let us consider that the registered sample paths are expressed in terms of basis functions as in 2 and let us denote by $A = (a_{ij})_{n \times p}$ the matrix of basis coefficients. Then, the principal component weight function \hat{f}_j^* admits the basis expansion

$$\hat{f}_j^*(u) = \sum_{k=1}^p b_{jk} \phi_k(u),$$

and FPCA is equivalent to multivariate PCA of matrix $A\Psi^{\frac{1}{2}}$ [51], with $\Psi^{\frac{1}{2}}$ being the squared root of the matrix of inner products between basis functions $\Psi := (\Psi_{ij})_{p \times p} := \int_T \phi_i(u) \phi_j(u) du$.

Then, the vector b_j of basis coefficients of the j -th principal weight function is given by $b_j = \Psi^{-\frac{1}{2}} u_j$, where the vectors u_j are computed as the solutions to the eigenvalue problem $n^{-1} \Psi^{\frac{1}{2}} A' A \Psi^{\frac{1}{2}} u_j = \lambda_j^* u_j$, where $n^{-1} \Psi^{\frac{1}{2}} A' A \Psi^{\frac{1}{2}}$ is the sample covariance matrix of $A\Psi^{\frac{1}{2}}$.

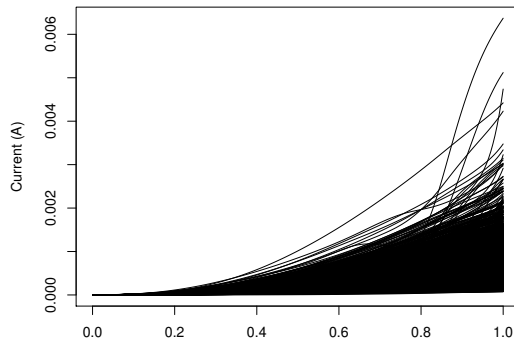


Figure 3: Sample of 3057 reset curves obtained for the same device under successive set-reset cycles registered in the interval $[0,1]$.

4. Results and discussion

In order to estimate the principal component decomposition of the reset process previously developed, we have a sample of 3057 reset current-voltage curves obtained for the same device under successive set-reset cycles

$$\{I_i(v) : i = 1, \dots, 3057\},$$

observed at the voltage points $v_j = j * 10^{-3}$ ($j = 1, \dots$) until the filament rupture that defines the end of the domain given by the reset voltage $V_{i-reset}$. FPCA of the reset process is estimated by following the three steps described in previous section. First, sample reset curves are registered in the interval $[0,1]$. All the registered curves are displayed in Figure 3. The sample mean function (left) next to pointwise confidence bands are displayed in Figure 4. Second, P-spline smoothing on the registered discrete data is performed for each of the reset curves in terms of a basis of cubic B-splines defined on 17 equally spaced knots in the interval $[0,1]$. And third, functional principal components are computed by multivariate PCA on the matrix of basic coefficients appropriately transformed.

The principal component weights associated with the first four principal

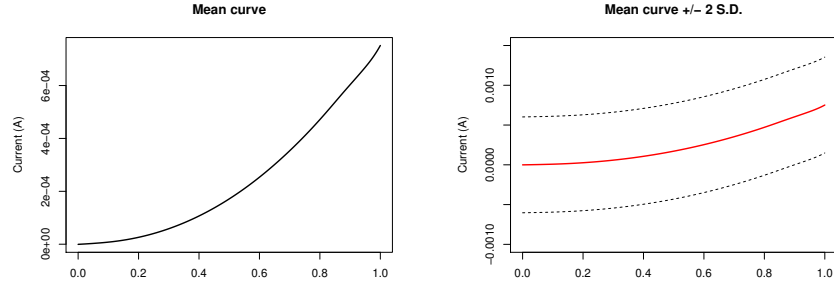


Figure 4: Functional mean of reset curves and confidence bands computed as ± 2 times the standard deviation at each current.

components are shown in Figure 5. The percentages of variance explained by the first four principal components are given in Table 1. Let us observe that only the first principal component explains more than a 97% of the total variability of the reset process. Because of this, the principal component decomposition of the registered reset curves can be truncated in the first term providing the following model:

$$I^{*1}(u) = \bar{I}^*(u) + \xi_1^* f_1^*(u), \quad u \in [0, 1],$$

where ξ_1^* is a scalar random variable (first principal component score) and f_1^* is a deterministic function (principal component weight curve). The accurated reconstruction given by this principal component decomposition can be seen in Figure 6 where some of the registered curves are approximated in terms of the first principal component. One of the main advantages of this simple linear representation of the reset process is that it could be used for circuit simulation if the distribution of probability of the first principal component is known.

In order to fit a probability model to the scores of the first principal component, the histogram of frequencies related to those scores can be seen in Figure 7 (left panel). This distribution presents a clear skewness to the left, and then some transformation should be considered in order to fit this data by a known

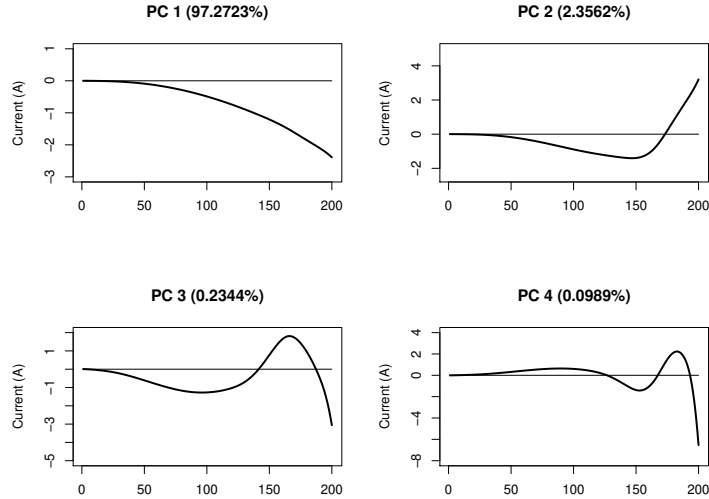


Figure 5: First four principal components weigh functions of the registered curves.

distribution. After some trials, the transformation $1/(\xi_1^* + 1)$ has been considered. The corresponding histogram of frequencies is shown in Figure 7 (right panel).

Taking into account the new transformed data, distributions such as Gamma or Log-normal have been considered without success.

Finally, a Gumbel distribution was considered so that the Kolmogorov-Smirnov goodness-of-fit test provides a $P - value = 0.06$. Then, with a significance level of 5%, a Gumbel distribution can be accepted to model the first p.c. scores. The ML estimation of its parameters is $\mu = 0.99992$, $\beta = 0.00014$, with μ and β being the location and scale parameters, respectively. This fit has been represented in Figure8.

5. Conclusions

Resistive Random Access Memories (RRAMs), based on the resistive switching of transition metal oxide films (TMOs), is one of the strongest candidates

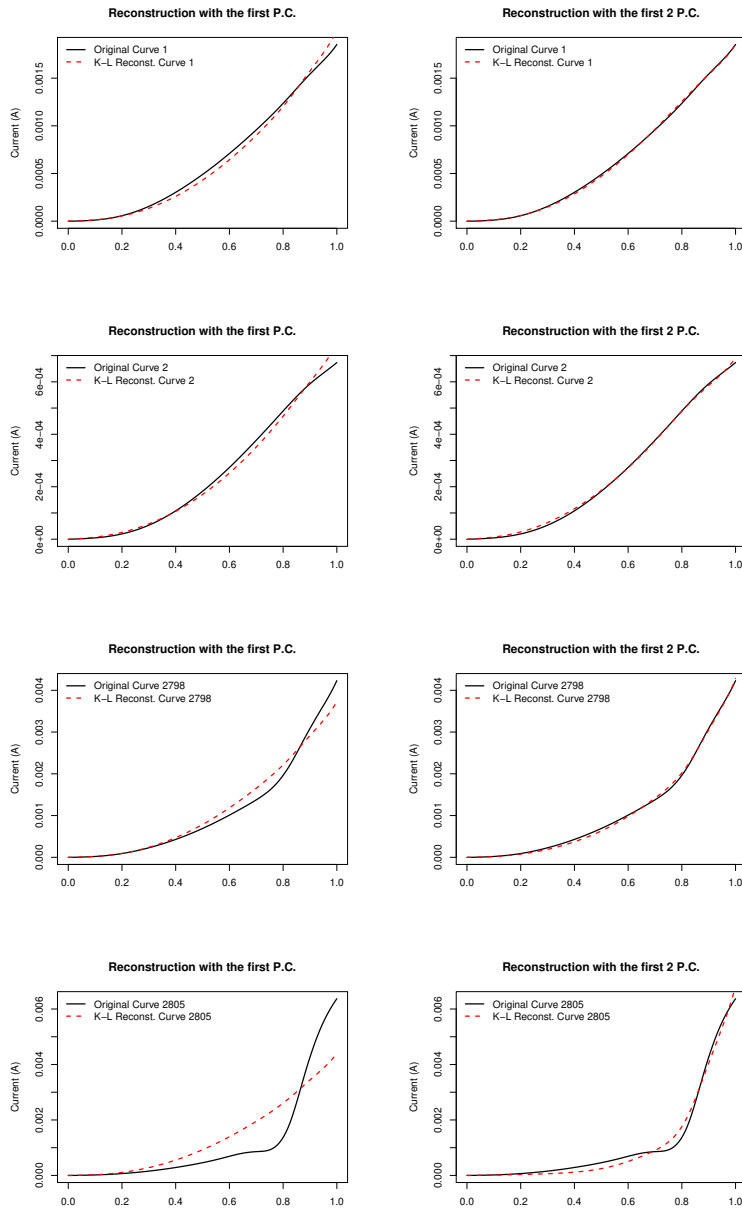


Figure 6: P-spline smoothing of some reset curves (black line) superposed with their reconstructions (red broken line) in terms of the first p.c. (left) and the first two pc's (right).

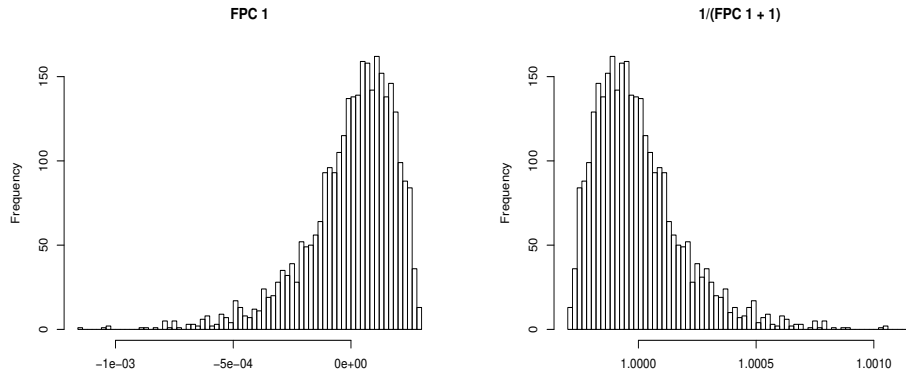


Figure 7: Histogram of absolute frequencies related to the scores of the first functional principal component with and without transformation (right and left panels, respectively).

for future nonvolatile applications due to their good scalability, long endurance, fast switching speed, and ease of integration in the back end of the line of CMOS processing.

This paper introduces a new method to model RRAM devices that can easily account for their current calculation and their statistical variability description. The methodology is based on a powerful tool of functional data analysis that allows the device current calculation making use of just one random parameter. A three step procedure based on curve registration, basis representation by P-spline smoothing and FPCA orthogonal decomposition, is developed. In this manner, previous complicated compact models for RRAMs can be simplified. In addition, variability, a key issue to take into consideration prior to industrial use of RRAMs, can be analyzed in an intuitive way, considering a probability function to describe accurately the distribution of the only parameter employed in the model. This new implementation represents a step forward in the simplicity-accuracy dilemma that is always presented in the compact modeling context since a reasonable accuracy has been obtained with just one parameter. Two random parameters can be used if a more restrictive fitting process is

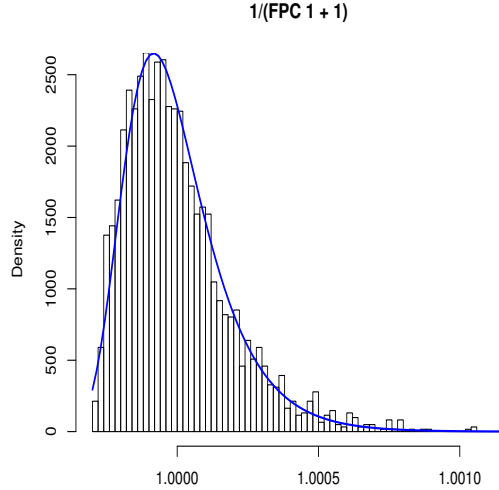


Figure 8: Density function fitted from a Gumbel distribution with parameters $\mu = 0.99992$, $\beta = 0.00014$, with μ and β being the location and scale parameters, respectively.

needed; nevertheless, two parameters is also a low number compared to the set of parameters employed in other modeling approaches. Further research studies focused on the physical meaning of this parameter and other higher order principal components can be easily performed by employing this new technique. Other lines of future research will be based on using advanced functional regression models (functional principal component and partial least squared regression [52], functional logit regression [53], functional analysis of variance [54], ...) for modelling important scalar variables related with the design of RRAM devices.

Acknowledgments

We thank the Spanish Ministry of Economy and Competitiveness for Projects MTM2017-88708-P and TEC2014-52152-C3-2-R (also supported by the FEDER program). We would like also to thank F. Campabadal and M. B. González from the IMB-CNM (CSIC) in Barcelona for fabricating and providing the experi-

mental measurements of the devices employed here.

References

References

- [1] G. Moore, Cramming more components onto integrated circuits, *Electronics Magazine* 38 (1965) 8.
- [2] Y. Xie, *Emerging Memory Technologies*, Springer, 2014.
- [3] R. Waser, M. Aono, Nanoionics-based resistive switching memories, *Nature materials* 6 (11) (2007) 833–840.
- [4] F. Pan, S. Gao, C. Chen, C. Song, F. Zeng, Recent progress in resistive random access memories: materials, switching mechanisms and performance, *Materials Science and Engineering* 24 (2014) 421.
- [5] J. Lee, S. Lee, T. Noh, Resistive switching phenomena: A review of statistical physics approaches, *Applied Physics Reviews* 2 (2015) 031303.
- [6] H.-S. P. Wong, S. Raoux, S. Kim, J. Liang, J. Reifenberg, B. Rajendran, M. Asheghi, K. Goodson, Phase change memory, *Proceedings of The IEEE - PIEEE* 98 (2010) 2201–2227.
- [7] W. Zhao, S. Chaudhuri, C. Accoto, J.-O. Klein, D. Ravelosona, C. Chappert, P. Mazoyer, High density spin-transfer torque (stt)-mram based on cross-point architecture, 4th IEEE International Memory Workshop (IMW) (2012) 1–4.
- [8] D. B. Strukov, G. S. Snider, D. R. Stewart, R. S. Williams, The missing memristor found, *Nature* 453 (7191) (2008) 80–83.
- [9] R. Picos, J. B. Roldán, M. N. Al Chawa, F. Jiménez-Molinos, M. A. Villena, E. García-Moreno, Exploring ReRAM-based memristors in the charge-flux domain, a modeling approach, in: *Proceedings of International Conference on Memristive Systems, MEMRISYS'2015*, 2015.

- [10] Z. Biolek, D. Biolek, V. Biolkova, Spice model of memristor with nonlinear dopant drift, *Radioengineering* 18 (2) (2009) 210–214.
- [11] F. Jiménez-Molinos, M. Villena, J. B. Roldán, A. M. Roldán, et al., A spice compact model for unipolar rram reset process analysis, *Electron Devices, IEEE Transactions on* 62 (3) (2015) 955–962.
- [12] S. Shin, K. Kim, S.-M. Kang, Compact models for memristors based on charge-flux constitutive relationships, *Computer-Aided Design of Integrated Circuits and Systems, IEEE Transactions on* 29 (4) (2010) 590–598.
- [13] J. O. Ramsay, B. W. Silverman, *Functional data analysis (Second Edition)*, Springer-Verlag, 2005.
- [14] J. O. Ramsay, B. W. Silverman, *Applied functional data analysis: Methods and case studies*, Springer-Verlag, 2002.
- [15] F. Ferraty, P. Vieu, *Nonparametric functional data analysis. Theory and practice*, Springer-Verlag, 2006.
- [16] J. O. Ramsay, G. Hooker, S. Graves, *Functional Data Analysis with R and MATLAB*, Springer-Verlag, 2009.
- [17] L. Horvath, P. Kokoszka, *Inference for functional data with applications*, Springer-Verlag, 2012.
- [18] J. C. Deville, Méthodes statistiques et numériques de l’analyse harmonique, *Annales de l’INSEE* 15 (1974) 3–101.
- [19] M. Loève, Analyse harmonique générale d’une fonction aléatoire, *Comptes Rendus de l’Académie des Sciences* 220 (1946) 380–382.
- [20] K. O. Karhunen, Zür spektraltheorie stochastischer prozesse, *Annales Academiae Scientiarum Fennicae, Ser. A* 34 (1946).
- [21] R. M. Fernández-Alcalá, J. Navarro-Moreno, J. Ruiz-Molina, Nonlinear estimation using correlation information, *IEEE Transactions on Signal Processing* in press (2006).

- [22] A. M. Aguilera, M. Escabias, C. Preda, G. Saporta, Using basis expansion for estimating functional PLS regression. Applications with chemometric data, *Chemometrics and Intelligent Laboratory Systems* 104 (2) (2010) 289–305.
- [23] P. Hall, D. Poskitt, B. Presnell, A functional data—analytic approach to signal discrimination, *Technometrics* 43(1) (2012) 1–9.
- [24] R. Zhou, N. Serban, N. Gebraeel, H.-G. Müller, A functional time warping approach to modeling and monitoring truncated degradation signals, *Technometrics* 56(1) (2013) 67–77.
- [25] B. Martin-Barragan, R. Lillo, J. Romo, Functional boxplots based on epigraphs and hypographs, *Journal of Applied Statistics* 43 (6) (2016) 1088–1103.
- [26] K. Chen, P. Delicado, H.-G. Müller, Modelling function-valued stochastic processes, with applications to fertility dynamics, *Journal of the Royal Statistical Society: Series B (Statistical Methodology)* 79(1) (2017) 177–196.
- [27] A. Menafoglio, M. Grasso, P. Secchi, B. Colosimo, Profile monitoring of probability density functions via simplicial functional pca with application to image data, *Technometrics* 56(1) (2013) 67–77.
- [28] J. Portela, A. Muñoz, E. Alonso, Forecasting functional time series with a new hilbertian armax model: application to electricity price forecasting, *IEEE Transactions on Power Systems* 33 (1) (2018) 545–556.
- [29] A. M. Aguilera, M. C. Aguilera-Morillo, Penalized PCA approaches for B-spline expansions of smooth functional data, *Applied Mathematics and Computation* 219 (14) (2013) 7805–7819.
- [30] M. González, J. Rafí, O. Beldarrain, M. Zabala, F. Campabadal, Analysis of the switching variability in Ni/HfO₂-based RRAM devices, *Device and Materials Reliability, IEEE Transactions on* 14 (2) (2014) 769–771.

- [31] M. Villena, F. Jiménez-Molinos, J. Roldán, J. Suñé, S. Long, X. Lian, F. Gámiz, M. Liu, An in-depth simulation study of thermal reset transitions in resistive switching memories, *Journal of Applied Physics* 114 (14) (2013) 144505.
- [32] M. Villena, M. González, F. Jiménez-Molinos, F. Campabadal, J. Roldán, J. Suñé, E. Romera, E. Miranda, Simulation of thermal reset transitions in resistive switching memories including quantum effects, *Journal of Applied Physics* 115 (21) (2014) 214504.
- [33] M. Villena, M. González, J. Roldán, F. Campabadal, F. Jiménez-Molinos, F. Gómez-Campos, J. Suñé, An in-depth study of thermal effects in reset transitions in HfO₂ based rrams, *Solid-State Electronics* 111 (2015) 47–51.
- [34] M. Villena, J. Roldán, M. González, P. González-Rodelas, F. Jiménez-Molinos, F. Campabadal, D. Barrera, A new parameter to characterize the charge transport regime in Ni/HfO₂/Si-n+ based rrams, *Solid-State Electronics* 118 (2016) 56–60.
- [35] J. C. Deville, Estimation of the eigenvalues and of the eigenvectors of a covariance operator, *Note interne de l'INSEE* (1973).
- [36] J. Dauxois, A. Pousse, Y. Romain, Asymptotic theory for the principal component analysis of a vector random function: some applications to statistical inference, *Journal of Multivariate Analysis* 12 (1) (1982) 136–156.
- [37] G. Saporta, Méthodes exploratoires d'analyse de données temporelles, *Cahiers du B.U.R.O., Université Pierre et Marie Curie* (1981) 37–38.
- [38] A. M. Aguilera, R. Gutiérrez, M. J. Valderrama, Approximation of estimators in the PCA of a stochastic proces using B-splines, *Communications in Statistics. Simulation and Computation* 25 (3) (1996) 671–690.
- [39] A. M. Aguilera, M. Escabias, F. A. Ocaña, M. J. Valderrama, Functional Wavelet-Based Modelling of Dependence Between Lupus and

- Stress, Methodology and Computing in Applied Probability 17 (4) (2015) 1015–1028.
- [40] C. De Boor, A practical guide to splines (revised edition), Springer, 2001.
- [41] W. Svante, Spline functions in data analysis, Technometrics 16(1) (1974) 1–11.
- [42] C. De Boor, Package for calculating with B-splines, Journal of Numerical Analysis 14 (3) (1977) 441–472.
- [43] M. Ibáñez, J. Roldán, A. Roldán, R. Yáñez, A comprehensive characterization of the threshold voltage extraction in mosfets transistors based on smoothing splines, Mathematics and Computers in Simulation 102 (2014) 1–10.
- [44] P. González, M. Ibáñez, A. Roldán, J. Roldán, An in-depth study on weno-based techniques to improve parameter extraction procedures in mosfet transistors, Mathematics and Computers in Simulation 118 (2015) 248–257.
- [45] P. H. C. Eilers, B. D. Marx, Flexible smoothing with B-splines and penalties, Statistical Science 11 (2) (1996) 89–121.
- [46] P. Eilers, B. Marx, M. Durbán, Twenty years of p-splines, SORT 39 (2015) 149–186.
- [47] A. M. Aguilera, M. C. Aguilera-Morillo, Comparative study of different B-spline approaches for functional data, Mathematical and Computer Modelling 58 (7-8) (2013) 1568–1579.
- [48] P. Craven, G. Wahba, Smoothing noisy data with spline functions - Estimating the correct degree of smoothing by the method of generalized cross-validation, Numerische Mathematik 31 (4) (1978) 377–403.

- [49] B. Brumback, J. Rice, Smoothing spline models for the analysis of nested and crossed samples of curves, *Journal of the American Statistical Association* 93 (1998) 961–994.
- [50] P. Craven, G. Wahba, The analysis of designed experiments and longitudinal data using smoothing splines, *Applied Statistics* 48 (1999) 269–312.
- [51] F. A. Ocaña, A. M. Aguilera, M. Escabias, Computational considerations in functional principal component analysis, *Computational Statistics* 22 (3) (2007) 449–465.
- [52] A. M. Aguilera, M. C. Aguilera-Morillo, C. Preda, Penalized versions of functional pls regression, *Chemometrics and Intelligent Laboratory Systems* 154 (2016) 80–92.
- [53] M. C. Aguilera-Morillo, A. M. Aguilera, M. Escabias, M. J. Valderrama, Penalized spline approaches for functional logit regression, *TEST* 22 (2) (2013) 251–277.
- [54] J.-T. Zhang, *Analysis of Variance for functional data*, CRC Press, 2014.